

# Particle number renormalization in almost half filled Mott Hubbard superconductors

Bernhard Edegger<sup>1</sup>, Noboru Fukushima<sup>2</sup>, Claudius Gros<sup>1</sup>, V.N. Muthukumar<sup>3</sup>

<sup>1</sup> Institute for Theoretical Physics, Universität Frankfurt, D-60438 Frankfurt, Germany

<sup>2</sup> Department of Physics, University of the Saarland, D-66041 Saarbrücken, Germany and

<sup>3</sup> Department of Physics, City College of the City University of New York, New York, NY 10031

(Dated: March 1, 2019)

The effects of the Gutzwiller projection on a BCS wave function with varying particle number are considered. We show that a fugacity factor has to be introduced in these wave functions when they are Gutzwiller projected, and derive an expression for this factor within the Gutzwiller approximation. We examine the effects of the projection operator on BCS wave functions by calculating the average number of particles before and after projection. We also calculate particle number fluctuations in a projected BCS state. Finally, we point out the differences between projecting BCS wave functions in the micro and grand canonical schemes, and discuss the relevance of our results for variational Monte Carlo studies.

PACS numbers: 74.20.-z, 74.20.Mn

## I. INTRODUCTION

Recently, Anderson has underscored the importance of fugacity in wave functions that do not conserve particle number<sup>1</sup>. Following an earlier paper by Laughlin<sup>2</sup>, Anderson argued that a fugacity factor should be included in variational wave functions of the form,

$$P |\Psi_{\text{BCS}}\rangle = P \prod_k \left( u_k + v_k c_{k\uparrow}^\dagger c_{-k\downarrow}^\dagger \right) |0\rangle. \quad (1)$$

Here,  $P = \prod_i (1 - n_{i\uparrow} n_{i\downarrow})$  is a (Gutzwiller) projection operator which excludes double occupancies at sites  $i$  (Ref. 3), and  $|\Psi_{\text{BCS}}\rangle$ , a BCS wave function. Projected wave functions of this form were originally proposed to describe the phase diagram of doped Mott Hubbard insulators such as the high temperature superconductors<sup>4,5,6</sup>. Detailed variational Monte Carlo (VMC) studies have been carried out recently using projected  $d$ -wave BCS states as variational wave functions for the two dimensional Hubbard model, after a suitable canonical transformation<sup>7,8</sup>.

Despite their simple form, projected wave functions exhibit nontrivial properties because the projection operator acts on a quantum many body state. The action of the projection operator (in reducing the allowed states in the Hilbert space) concomitant with the correlations of the quantum state being projected, leads to a variety of physical phenomena<sup>9</sup>. Other interesting effects include non-trivial matrix-element renormalization near half-filling<sup>10</sup> and the occurrence of superconductivity near an antiferromagnetic Mott insulator<sup>11</sup>.

Approximate analytical calculations with wave functions such as Eq. (1) can be done using a renormalization scheme based on the Gutzwiller approximation. Within this approximation, the effects of projection on the state  $|\Psi_0\rangle$  are approximated by a classical statistical weight factor multiplying the quantum result<sup>12,13</sup>. Thus, for ex-

ample,

$$\frac{\langle \Psi | \hat{O} | \Psi \rangle}{\langle \Psi | \Psi \rangle} \approx g \frac{\langle \Psi_0 | \hat{O} | \Psi_0 \rangle}{\langle \Psi_0 | \Psi_0 \rangle}, \quad (2)$$

where  $\hat{O}$  is any operator, and  $g$ , the so called Gutzwiller factor. For example, the Gutzwiller approximation for the kinetic energy operator  $c_i^\dagger c_j + c_j^\dagger c_i$  and the superexchange interaction between sites  $i$  and  $j$ ,  $\vec{S}_i \cdot \vec{S}_j$  yields the Gutzwiller factors,

$$g_t = \frac{1-n}{1-n/2}, \quad g_s = \frac{1}{(1-n/2)^2}, \quad (3)$$

where  $n$  is the density of electrons. In deriving these renormalization factors, one considers the number of terms that contribute to  $\langle \Psi | \hat{O} | \Psi \rangle$  and to  $\langle \Psi_0 | \hat{O} | \Psi_0 \rangle$  respectively. The ratio of these two contributions is the renormalization factor.

The renormalization factors are functions of the *local* charge density. This is a well defined quantity when one considers for example, a projected Fermi liquid state,

$$P |\Psi_{\text{FS}}\rangle = P \prod_{k < k_F} c_{k\uparrow}^\dagger c_{k\downarrow}^\dagger |0\rangle. \quad (4)$$

But suppose instead, we consider wave functions such as the BCS state in Eq. (1), where the particle number fluctuates. In this case, it is not clear what the local charge density in Eq. (3) should be. It may be argued that the correct  $n$  is set by the average particle number  $\bar{N}$ . But then, projecting a BCS state changes the average particle number; *i.e.*, the average number of electrons in  $|\Psi_{\text{BCS}}\rangle$  does not equal that in  $P|\Psi_{\text{BCS}}\rangle$ . Clearly, we need a scheme to keep track of this effect.

Note that this problem can be avoided completely, as is done in most variational Monte Carlo (VMC) studies. Here, the particle number is fixed (one works in a micro canonical ensemble), and Eq. (1) replaced by,

$$P_N P |\Psi_{\text{BCS}}\rangle = P_N P \prod_k \left( u_k + v_k c_{k\uparrow}^\dagger c_{-k\downarrow}^\dagger \right) |0\rangle. \quad (5)$$

The operator  $P_N$  fixes the particle number, and the issue of projection changing the mean particle number does not arise<sup>4</sup>. However, there are also other VMC studies with wave functions that do not have fixed particle number<sup>14</sup>. In addition, we are often interested in carrying out analytical approximations in the spirit of Eq. (2). Since such manipulations are easier done with BCS wave functions (where the particle number is not fixed), it is desirable to understand the effects of the projection operator on this class of wave functions. In this paper, we present analytical and numerical considerations of this problem. In doing so, we clarify the notion of fugacity introduced by Anderson<sup>1</sup>. We also discuss the relevance of this approach for the Gutzwiller approximation in the grand canonical scheme and the corresponding VMC studies<sup>14</sup>.

## II. THE FUGACITY FACTOR

Consider the projected BCS wave function, Eq. (1). It is clear that the projection operator  $P$  changes the average number; *viz.*,

$$\frac{\langle \Psi_{\text{BCS}} | \hat{N} | \Psi_{\text{BCS}} \rangle}{\langle \Psi_{\text{BCS}} | \Psi_{\text{BCS}} \rangle} \neq \frac{\langle \Psi_{\text{BCS}} | P \hat{N} P | \Psi_{\text{BCS}} \rangle}{\langle \Psi_{\text{BCS}} | P^2 | \Psi_{\text{BCS}} \rangle}.$$

The effect of the projection operator can be seen most clearly by examining the particle number distribution in the unprojected and projected Hilbert spaces. Towards this end, let us write the average numbers,  $\bar{N}^{(0)}(\bar{N})$  in the unprojected (projected) Hilbert space

$$\bar{N}^{(0)} = \sum_N N \rho_N^{(0)}, \quad (6)$$

$$\bar{N} = \sum_N N \rho_N. \quad (7)$$

Here,

$$\begin{aligned} \rho_N^{(0)} &= \frac{\langle \Psi_{\text{BCS}} | P_N | \Psi_{\text{BCS}} \rangle}{\langle \Psi_{\text{BCS}} | \Psi_{\text{BCS}} \rangle}, \\ \rho_N &= \frac{\langle \Psi_{\text{BCS}} | P P_N P | \Psi_{\text{BCS}} \rangle}{\langle \Psi_{\text{BCS}} | P P | \Psi_{\text{BCS}} \rangle}, \end{aligned}$$

are the particle number distributions in the unprojected and projected BCS wave functions respectively;  $P_N$  is an operator which projects onto terms with particle number  $N$ . The particle number distributions before and after projection may be related by

$$\underbrace{\frac{\langle \Psi_{\text{BCS}} | P P_N P | \Psi_{\text{BCS}} \rangle}{\langle \Psi_{\text{BCS}} | P P | \Psi_{\text{BCS}} \rangle}}_{\rho_N} = g_N \underbrace{\frac{\langle \Psi_{\text{BCS}} | P_N | \Psi_{\text{BCS}} \rangle}{\langle \Psi_{\text{BCS}} | \Psi_{\text{BCS}} \rangle}}_{\rho_N^{(0)}}, \quad (8)$$

where

$$g_N = \underbrace{\frac{\langle \Psi_{\text{BCS}} | \Psi_{\text{BCS}} \rangle}{\langle \Psi_{\text{BCS}} | P P | \Psi_{\text{BCS}} \rangle}}_{=C(\text{const})} \frac{\langle \Psi_{\text{BCS}} | P P_N P | \Psi_{\text{BCS}} \rangle}{\langle \Psi_{\text{BCS}} | P_N | \Psi_{\text{BCS}} \rangle}.$$

Eq. (8) constitutes the Gutzwiller approximation for the projection operator  $P_N$  with the corresponding renormalization factor,  $g_N$ ;  $C$  is an irrelevant constant (the ratio of the normalization of the unprojected and projected wave functions), which does not depend on  $N$ . Following Gutzwiller, we estimate  $g_N$  by combinatorial means, as being equal to the ratio of the relative sizes of the projected and unprojected Hilbert spaces. Then,

$$g_N \approx C \frac{\frac{L!}{(L-N_{\uparrow}-N_{\downarrow})! N_{\uparrow}! N_{\downarrow}!}}{\frac{L!}{(L-N_{\uparrow})! N_{\uparrow}!} \frac{L!}{(L-N_{\downarrow})! N_{\downarrow}!}}, \quad (9)$$

where  $L$  is the number of lattice sites and  $N_{\uparrow}$  ( $N_{\downarrow}$ ) is the number of up (down)-spins. Since in a BCS wave function,  $N_{\uparrow} = N_{\downarrow} = N/2$ ,  $N$  being the total number of particles, the expression for  $g_N$  can be simplified to

$$g_N \approx C \frac{((L-N/2)!)^2}{L! (L-N)!}. \quad (10)$$

Hence, if we were to impose the condition that the average particle number before and after projection be identical, a factor  $g_N^{-1}$  has to be included in Eq. (7). Then, from Eq. (7) and Eq. (8), we obtain the particle number after projection  $\bar{N}_{\text{new}}$ ,

$$\begin{aligned} \bar{N}_{\text{new}} &\equiv \sum_N N \frac{1}{g_N} \rho_N = \sum_N N \frac{g_N \rho_N^{(0)}}{g_N} \\ &= \bar{N}^{(0)}, \end{aligned} \quad (11)$$

which is the desired result.

Now, let us show how this procedure can be implemented for the wave function  $|\Psi_{\text{BCS}}\rangle$ . Since the BCS wave function is a linear superposition of states with particle number  $\dots, N-2, N, N+2, \dots$ , we consider the effect of projection on two states whose particle numbers differ by 2. Then, the ratio,

$$f^2 \equiv \frac{g_{N+2}}{g_N} \approx \left( \frac{L-N}{L-N/2} \right)^2, \quad (12)$$

in the thermodynamic limit. Eq. 12 shows that the projection operator acts unequally on the  $N$  and  $N+2$  particle states; the renormalization of the weight of the  $N+2$  particle states  $g_{N+2}$ , is  $f^2$  times the weight of the  $N$  particle states,  $g_N$ . This effect can be rectified as in Eq. (11) by multiplying every Cooper pair  $c_{k\uparrow}^{\dagger} c_{-k\downarrow}^{\dagger}$  by a factor  $\frac{1}{f}$  in the BCS wave function. It produces the desired result, *viz.*, the projected and unprojected BCS wave functions have the same average particle number.

Alternatively (following Anderson), we can multiply every empty state by the factor  $f$  and write,

$$|\Psi_{\text{BCS}}^{(f)}\rangle = \prod_k \frac{\left( f u_k + v_k c_{k\uparrow}^{\dagger} c_{-k\downarrow}^{\dagger} \right)}{\sqrt{f^2 |u_k|^2 + |v_k|^2}} |0\rangle. \quad (13)$$

Then again by construction, the fugacity factor  $f$  in Eq. (13) ensures that the projected wave function

$P|\Psi_{\text{BCS}}^{(f)}\rangle$  and the unprojected wave function  $|\Psi_{\text{BCS}}\rangle$  have the same particle number. The denominator in Eq. (13) is the new normalization factor.

The following points are in order: (a) the fugacity factor  $f$  in Eq. (12) depends on the variable particle number  $N$ . However, since the particle number of the BCS wave function is sharply peaked within the range,  $\bar{N}^{(0)} - \sqrt{\bar{N}^{(0)}}$  and  $\bar{N}^{(0)} + \sqrt{\bar{N}^{(0)}}$ , we will assume that the fugacity factor  $f = f(\bar{N}^{(0)})$  in the thermodynamic limit; (b) in this limit, Eq. (12) reduces to  $f^2 = g_t^2$ , where  $g_t$  is the Gutzwiller factor defined in Eq. (3). Then, Eq. (13) reduces to

$$|\Psi_{\text{BCS}}^{(f)}\rangle = \prod_k \frac{\left(g_t u_k + v_k c_{k\uparrow}^\dagger c_{-k\downarrow}^\dagger\right)}{\sqrt{g_t^2 |u_k|^2 + |v_k|^2}} |0\rangle, \quad (14)$$

which is the wave function proposed by Anderson<sup>1</sup>; (c) the fugacity factor ensures that projection affects the  $N$  and  $N+2$  particle states of the BCS wave function in the same way. In principle, such a factor could depend on the  $k$ -value, but in this paper, we will treat it as a mere combinatorial device; (d) the combinatorial argument fails at half filling when  $L = \bar{N}^{(0)}$ .

### III. PARTICLE NUMBER RENORMALIZATION IN PROJECTED BCS WAVE FUNCTIONS

In the previous section, we showed that the inclusion of the fugacity factor is necessary for the average particle number in a BCS wave function to be unchanged by projection. Alternatively, one might ask what is the effect of the projection operator on a BCS wave function; *viz.*, if projection changes the mean particle number of a BCS state, how are the particle numbers before and after projection related? In this section, we will use the fugacity factor to answer this question. In particular, we will show how particle density after projection can be determined self consistently by including the fugacity factor in the projected BCS state (Eq. (14)). An alternate derivation of this result is presented in Appendix A, where the effect of the projection operator on particle number fluctuations is calculated.

Consider two BCS states defined by

$$|\Psi_{\text{BCS}}\rangle = \prod_k \left(u_k + v_k c_{k\uparrow}^\dagger c_{-k\downarrow}^\dagger\right) |0\rangle, \quad (15)$$

$$\begin{aligned} |\Psi_{\text{BCS}}^{(r)}\rangle &= \prod_k \frac{\left(u_k + g_t v_k c_{k\uparrow}^\dagger c_{-k\downarrow}^\dagger\right)}{\sqrt{|u_k|^2 + g_t^2 |v_k|^2}} |0\rangle \\ &= \prod_k \left(u_k^{(r)} + v_k^{(r)} c_{k\uparrow}^\dagger c_{-k\downarrow}^\dagger\right) |0\rangle, \end{aligned} \quad (16)$$

where,

$$u_k^{(r)} \equiv \frac{u_k}{\sqrt{|u_k|^2 + g_t^2 |v_k|^2}}, \quad (17)$$

$$v_k^{(r)} \equiv \frac{g_t v_k}{\sqrt{|u_k|^2 + g_t^2 |v_k|^2}}. \quad (18)$$

From Eq. (12), it is clear that the projection operator reduces the ratio of the weights of  $N+2$  and  $N$  particle states in a BCS wave function by a factor  $g_t$ . Then, it follows that

$$\frac{\langle \Psi_{\text{BCS}}^{(r)} | \hat{N} | \Psi_{\text{BCS}}^{(r)} \rangle}{\langle \Psi_{\text{BCS}}^{(r)} | \Psi_{\text{BCS}}^{(r)} \rangle} \approx \frac{\langle \Psi_{\text{BCS}} | P \hat{N} P | \Psi_{\text{BCS}} \rangle}{\langle \Psi_{\text{BCS}} | P | \Psi_{\text{BCS}} \rangle} \quad (19)$$

when

$$g_t = \frac{L - \bar{N}^{(r)}}{L - \bar{N}^{(r)}/2}. \quad (20)$$

The average particle number  $\bar{N}^{(r)}$  of the state  $|\Psi_{\text{BCS}}^{(r)}\rangle$  is given by,

$$\bar{N}^{(r)} = \frac{\langle \Psi_{\text{BCS}}^{(r)} | \hat{N} | \Psi_{\text{BCS}}^{(r)} \rangle}{\langle \Psi_{\text{BCS}}^{(r)} | \Psi_{\text{BCS}}^{(r)} \rangle} = 2 \sum_k |v_k^{(r)}|^2. \quad (21)$$

Since the particle numbers of  $|\Psi_{\text{BCS}}^{(r)}\rangle$  and  $P|\Psi_{\text{BCS}}\rangle$  are identical, we can use Eq. (18) in Eq. (21) to obtain,

$$\begin{aligned} \bar{N}^{(r)} &\approx \bar{N}_{\text{after}} = \frac{\langle \Psi_{\text{BCS}} | P \hat{N} P | \Psi_{\text{BCS}} \rangle}{\langle \Psi_{\text{BCS}} | P | \Psi_{\text{BCS}} \rangle} \\ &\approx 2 \sum_k \frac{g_t^2 |v_k|^2}{|u_k|^2 + g_t^2 |v_k|^2}. \end{aligned} \quad (22)$$

Note that  $g_t$  is specified by the particle number after projection,  $N_{\text{after}}$  ( $= \bar{N}^{(r)}$ ).

Now, since the number of particles in the state  $|\Psi_{\text{BCS}}\rangle$  before projection is given by

$$\bar{n}_{\text{before}} = 2 \sum_k |v_k|^2,$$

Eq. (22) provides us with a way to calculate the number of particles in the state  $P|\Psi_{\text{BCS}}\rangle$  after projection, if  $|\Psi_{\text{BCS}}\rangle$  (*i.e.*,  $u_k$  and  $v_k$ ) is specified *before* projection. Eq. (22) can be solved self consistently for  $\bar{N}_{\text{after}}$ . We solve Eq. (22) numerically on a square lattice, using the standard BCS expressions for a  $d$ -wave superconductor,  $u_k(v_k)$ :

$$v_k^2 = \frac{1}{2} \left(1 - \frac{\xi_k}{E_k}\right), \quad (23)$$

$$u_k^2 = \frac{1}{2} \left(1 + \frac{\xi_k}{E_k}\right), \quad (24)$$

where,

$$E_k = (\Delta_k^2 + \xi_k^2)^{\frac{1}{2}}, \quad (25)$$

$$\Delta_k = \Delta_0 (\cos(k_x) - \cos(k_y)), \quad (26)$$

$$\xi_k = -2 (\cos(k_x) + \cos(k_y)) - \mu. \quad (27)$$

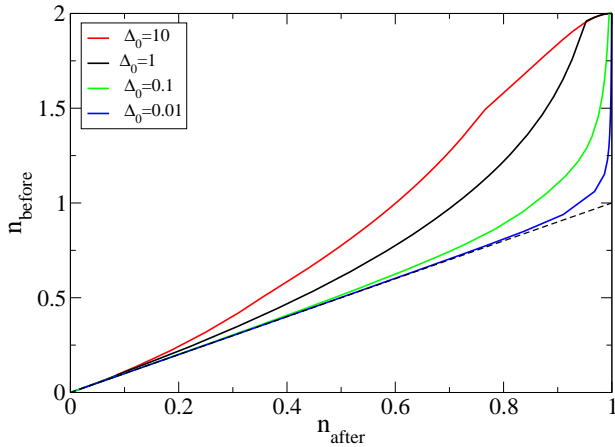


FIG. 1: Particle density before projection  $n_{\text{before}}$  as a function of the particle density after projection  $n_{\text{after}}$  for different  $d$ -wave order parameters  $\Delta_0$ . The dashed line indicates the Fermi liquid result  $n_{\text{before}} = n_{\text{after}}$ .

The only free parameters are the chemical potential  $\mu$  and the order parameter  $\Delta_0$ .

By fixing the order parameter  $\Delta_0$ , we determine the particle numbers (before and after projection) for various chemical potentials. The results for particle density ( $n \equiv \bar{N}/L$ ) are shown in Fig. 1. The results clearly show that the particle density before projection attains its maximal value ( $n_{\text{before}} = 2$ ), if  $n_{\text{after}} = 1$  (half-filling). This result holds for any finite value of the order parameter  $\Delta_0$ . In the opposite limit, *viz.*, low density of electrons,  $n_{\text{before}}$  converges to the value of  $n_{\text{after}}$  as expected. The size of the intermediate region depends on the magnitude of the order parameter  $\Delta_0$ , as illustrated by the results in Fig. 1.

The accuracy of Eq. (22) can be checked by comparing our results with those of Yokoyama and Shiba (YS), who performed VMC studies of projected BCS wave functions with fluctuating particle number (but without the fugacity factor)<sup>14</sup>. They determined the particle density of the projected  $d$ -wave state  $P|\Psi_{\text{BCS}}\rangle$  as a function of the chemical potential  $\mu$  and the order parameter  $\Delta_0$ , within a grand canonical scheme. The unprojected wave function  $|\Psi_{\text{BCS}}\rangle$  is specified as usual, through Eq. (23)-Eq. (27). Since YS do not include a fugacity factor in their definition of the BCS wave function, projection changes the particle number. So, we use Eq. (22) to determine  $n_{\text{after}}$  which we compare with their results for particle number.

As seen in Fig. 2, our results are in good qualitative agreement with YS. Discrepancies are mostly due to finite corrections. YS use  $6 \times 6$  and  $8 \times 8$ -lattices, while our analytic calculations are for the thermodynamic limit<sup>15</sup>. The results show the singular effect of the projection near the insulating phase (half filling). The chemical potential goes to infinity in this limit.

In Appendix A, we present an alternate derivation of Eq. (22) by a saddle point approximation without using

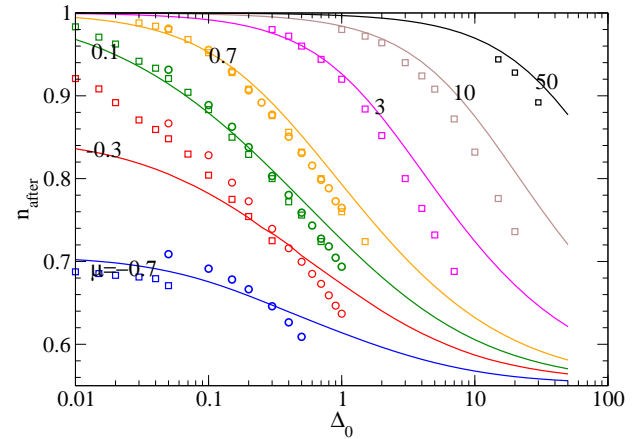


FIG. 2: The particle density after projection  $n_{\text{after}}$  as a function of the SC-order parameter  $\Delta_0$  for a  $d$ -wave BCS state at various chemical potentials  $\mu$ . The figure shows a comparison between results from Eq. (22)(solid lines) and the VMC results of Yokoyama and Shiba<sup>14</sup> (for  $6 \times 6$  - (circles) and  $8 \times 8$  -lattices (squares)). Numbers in the figure denote the chemical potentials of the corresponding curves.

a fugacity-corrected wave function. This approach also allows for the calculation of particle number fluctuations  $\sigma^2/L$ .

#### IV. GUTZWILLER APPROXIMATION IN THE MICRO- AND GRAND- CANONICAL SCHEMES

In this section, we discuss the differences between the Gutzwiller approximation in the micro- and grand-canonical schemes. The validity of our statements can be checked by a comparison to nearly exact VMC<sup>4,7,14</sup>.

Let us first consider the micro canonical case. Here, we are interested in the expectation value of an operator  $\hat{O}$  calculated with a particle number conserving projected wave function  $P_N P |\Psi_{\text{BCS}}\rangle$ . The corresponding Gutzwiller approximation can be understood as follows:

$$\begin{aligned} & \frac{\langle \Psi_{\text{BCS}} | P P_N \hat{O} P_N P | \Psi_{\text{BCS}} \rangle}{\langle \Psi_{\text{BCS}} | P P_N P | \Psi_{\text{BCS}} \rangle} \\ & \approx g \frac{\langle \Psi_{\text{BCS}} | P_N \hat{O} P_N | \Psi_{\text{BCS}} \rangle}{\langle \Psi_{\text{BCS}} | P_N | \Psi_{\text{BCS}} \rangle} \\ & = g \frac{\langle \Psi_{\text{BCS}} | \hat{O} | \Psi_{\text{BCS}} \rangle}{\langle \Psi_{\text{BCS}} | \Psi_{\text{BCS}} \rangle}, \end{aligned} \quad (28)$$

where  $P_N$  is the projector on the terms with particle number  $N$ . The Gutzwiller factor  $g$ , corresponds to the operator  $\hat{O}$ . The first row represents a quantity which can be calculated exactly by fixed particle number VMC<sup>4,7</sup>. Since the particle number is fixed, the Gutzwiller approximation can be invoked, leading to the second row. The equality to the third row is guaranteed only if  $N$  is equal to the average particle number of  $|\Psi_{\text{BCS}}\rangle$  ( $N = \bar{N}$ ).

Here, we perform a transformation from a micro canonical to a grand canonical ensemble, which is valid in the thermodynamic limit.

In the grand canonical scheme, where we calculate the expectation value of  $\hat{O}$  with a particle number non-conserving wave function, this scheme must be modified as follows:

$$\frac{\langle \Psi_{\text{BCS}}^{(f)} | P \hat{O} P | \Psi_{\text{BCS}}^{(f)} \rangle}{\langle \Psi_{\text{BCS}}^{(f)} | P P | \Psi_{\text{BCS}}^{(f)} \rangle} \approx g \frac{\langle \Psi_{\text{BCS}} | \hat{O} | \Psi_{\text{BCS}} \rangle}{\langle \Psi_{\text{BCS}} | \Psi_{\text{BCS}} \rangle}, \quad (29)$$

where  $P | \Psi_{\text{BCS}}^{(f)} \rangle$  is the projected  $d$ -wave state corrected for fugacity, *i.e.*, a fugacity factor is included simultaneously with the projection (see Sec. II). This correction is essential to guarantee the validity of the Gutzwiller approximation; without it, the lhs and rhs of Eq. (29) would correspond to states with different particle numbers.

Comparing Eq. (28) and Eq. (29) we get,

$$\frac{\langle \Psi_{\text{BCS}} | P P_N \hat{O} P_N P | \Psi_{\text{BCS}} \rangle}{\langle \Psi_{\text{BCS}} | P P_N P | \Psi_{\text{BCS}} \rangle} \approx \frac{\langle \Psi_{\text{BCS}}^{(f)} | P \hat{O} P | \Psi_{\text{BCS}}^{(f)} \rangle}{\langle \Psi_{\text{BCS}}^{(f)} | P^2 | \Psi_{\text{BCS}}^{(f)} \rangle}. \quad (30)$$

Eq. (29) and Eq. (30) constitute the main results of this section. Eq. (29) shows that when the Gutzwiller approximation is used for a wave function which does not have a fixed particle number, a fugacity factor must be included along with the projection. Eq. (30) shows that to obtain identical results, one has to use different wave functions in the grand canonical (rhs) and micro canonical (lhs) schemes. The wave function  $|\Psi_{\text{BCS}}^{(f)}\rangle$  is a  $d$ -wave state corrected by the fugacity factor, whereas  $|\Psi_{\text{BCS}}\rangle$  is a pure  $d$ -wave state. Our arguments leading up to Eq. (29) and Eq. (30) can be verified by a comparison with VMC studies. We now proceed to do so.

The expectation values in the micro- and grand- canonical schemes can be calculated (nearly exactly) by VMC studies. In Fig. 3, we show VMC results from Gros<sup>4</sup> (fixed particle number VMC, micro canonical) and from YS<sup>14</sup> (grand canonical VMC). The discrepancy between the two sets of results can be explained readily by Eq. (30). YS consider a pure  $d$ -wave state, *i.e.*, the fugacity factor is not included in their calculations. Eq. (30) on the other hand shows that this is only to be expected because the particle numbers in the two schemes are not identical without a fugacity factor. In their paper, YS argued that the discrepancies between the two results can be removed by introducing an additional variational parameter  $\alpha$ , so that  $a_k \equiv v_k/u_k$  is replaced by  $a_k \equiv \alpha v_k/u_k$  (Eq. 4.1 in Ref. 14). We opine that the parameter  $\alpha$  is directly related to our fugacity factor, *i.e.*,  $\alpha = g_t$  in the wave function  $|\Psi_{\text{BCS}}^{(f)}\rangle$ . This conclusion is supported by the comparison of VMC data to the corresponding Gutzwiller approximation (see below).

The validity of the approximation in the micro canonical case (Eq. (28)) is well accepted. It is used for instance, in the renormalized mean field theory (RMFT) of Zhang *et al.*, where all physical quantities are calculated

using unprojected wave functions and the corresponding Gutzwiller renormalization factors<sup>5</sup>. A comparison with VMC studies with fixed particle number exhibits a good agreement<sup>5</sup> (also illustrated in Fig. 3).

To compare the grand canonical VMC of YS with the Gutzwiller approximation, we need to modify Eq. (29). This is necessary because YS do not include the fugacity factor in their considerations, as pointed out earlier. We modify Eq. (30) by the following procedure:

- (i) we start with a  $d$ -wave BCS state  $|\Psi_{\text{BCS}}\rangle$  for specified values of  $\Delta_0$ ;
- (ii) we use Eq. (22) to determine the chemical potential  $\mu$ . This fixes the particle density  $n_{\text{after}}$  of  $P | \Psi_{\text{BCS}} \rangle$ ;
- (iii) we remove the fugacity factor to get  $|\Psi_{\text{BCS}}^{(r)}\rangle$  via Eq. (16). The fugacity factor is determined for  $n_{\text{after}}$ .  $|\Psi_{\text{BCS}}^{(r)}\rangle$  and  $P | \Psi_{\text{BCS}} \rangle$  correspond to the same particle density  $n_{\text{after}}$ .
- (iv) The expectation values of the wave function  $P | \Psi_{\text{BCS}} \rangle$  can now be approximated by  $|\Psi_{\text{BCS}}^{(r)}\rangle$  and Gutzwiller factors, *viz.*,

$$\frac{\langle \Psi_{\text{BCS}} | P \hat{O} P | \Psi_{\text{BCS}} \rangle}{\langle \Psi_{\text{BCS}} | P P | \Psi_{\text{BCS}} \rangle} \approx g \frac{\langle \Psi_{\text{BCS}}^{(r)} | \hat{O} | \Psi_{\text{BCS}}^{(r)} \rangle}{\langle \Psi_{\text{BCS}}^{(r)} | \Psi_{\text{BCS}}^{(r)} \rangle}. \quad (31)$$

This Gutzwiller approximation (GA) generalizes Eq. 2 for wave functions that do not conserve particle number. In Appendix B, we discuss this approximation for the different terms in the  $t - J$  model.

In Fig. 4, we compare the GA of the kinetic energy  $E^{(1)}$ , and the expectation value  $E^{(2)}$ , of the remaining terms in the  $t - J$  model ( $\langle \hat{S}_i \hat{S}_j \rangle$ ,  $\langle \hat{n}_i \hat{n}_j \rangle$ , and the 3-site term) to those from the grand canonical VMC. A good agreement between the VMC and Gutzwiller results is seen, which confirms the validity of our grand canonical Gutzwiller approximation (Eq. (29)).

In Fig. 3 and Fig. 4, we also show Gutzwiller approximations for the fixed particle number VMC<sup>4</sup>. Clearly, micro and grand canonical approaches yield different energies (as do the corresponding VMC studies). We emphasize this is because of the projection operator  $P$ , which changes the particle number in a grand canonical scheme. For these two methods to yield the same results, a fugacity corrected wave function must be used when working in a grand canonical ensemble. Hence, all previous speculations about the coincidence of these two VMC schemes in the thermodynamic limit (*e.g.*, Ref. 16) have to be reformulated carefully.

## V. SUMMARY

In this paper, we considered the effects of Gutzwiller projection on a state which does not have fixed particle number. We showed that it is necessary to include a fugacity factor when invoking the Gutzwiller approximation for such states. The effects of projecting a number non-conserving BCS state were studied by examining the

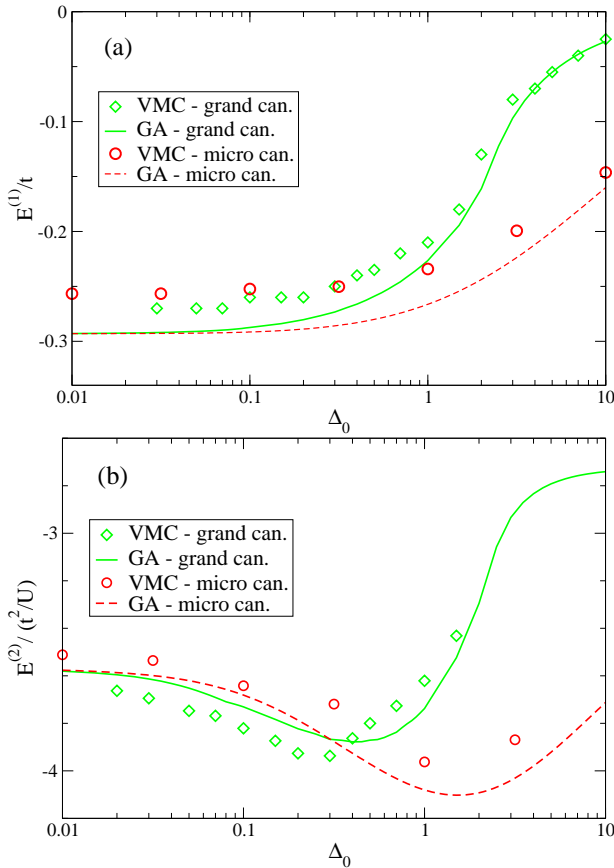


FIG. 3: (a) The kinetic energy  $E^{(1)}$  and (b) the energy of the remaining terms  $E^{(2)}$  per site of the  $t - J$  model as a function of  $\Delta_0$  for the  $d$ -wave state at a filling  $n = 0.9$ . Fixed particle (micro can.) VMC data<sup>4</sup> (circles, 82 sites) and grand canonical VMC<sup>14</sup> (squares,  $8 \times 8$  sites) are compared. The dashed/solid lines represent the corresponding Gutzwiller approximations (GA). For a detailed description, we refer to the text and Appendix B.

relation between particle number before and after projection. We obtained an analytical expression, Eq. (22), which was compared to variational Monte Carlo data (Fig. 2). We discussed the discrepancies in the VMC results for projected BCS wave functions obtained in the micro and grand canonical schemes, and presented a resolution. In conclusion, we have clarified several subtle properties of the Gutzwiller projection operator  $P$  acting on a BCS state, and hope that these results lead to a better understanding of the Gutzwiller approximation in the grand canonical scheme.

We thank P. W. Anderson, N. P. Ong, and H. Yokoyama for several discussions. N. F. was supported by the Deutsche Forschungsgemeinschaft. V. N. M. acknowledges partial financial support from The City University of New York, PSC-CUNY Research Award Program.

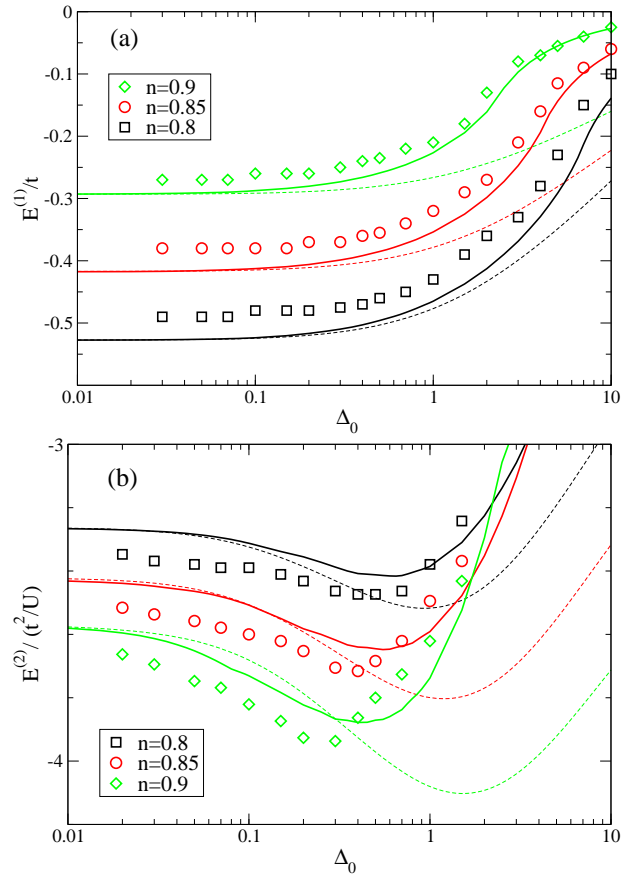


FIG. 4: (a) The kinetic energy  $E^{(1)}$  and (b) the energy of the remaining terms  $E^{(2)}$  per site of the  $t - J$  model, as a function of  $\Delta_0$  for the  $d$ -wave state at various densities. The data points (diamond, circle, square) are taken from the grand canonical VMC study of Yokoyama and Shiba<sup>14</sup>. The solid/dashed lines represent the Gutzwiller approximations for a grand canonical/fixed-particle VMC study. For a detailed description, we refer to the text and Appendix B.

#### APPENDIX A: SADDLE POINT APPROXIMATION TO MEAN PARTICLE NUMBER AND NUMBER FLUCTUATIONS IN PROJECTED BCS WAVE FUNCTIONS

In Sec. III, we used the fugacity factor to derive Eq. (22). Here, we present an alternative approach by a saddle point approximation to discuss the effects of projection on the mean particle number of a BCS state. This approach also describes the particle number fluctuations after projection.

The particle number distribution for an unprojected BCS wave function  $\rho_N^{(0)}$  can be written as

$$\rho_N^{(0)} = \frac{2}{N_\sigma!} \left( \frac{d}{d\lambda} \right)^{N_\sigma} \prod_k (|u_k|^2 + |v_k|^2 \lambda) \Big|_{\lambda=0}, \quad (A1)$$

where  $N_\sigma = N/2$  is the number of electron pairs. This relation can be checked by expanding the product in the

wave function,

$$|\Psi_{\text{BCS}}\rangle = \prod_k \left( u_k + v_k c_{k,\uparrow}^\dagger c_{-k,\downarrow}^\dagger \right) |0\rangle ,$$

and considering contribution to  $\langle \Psi_{\text{BCS}} | \Psi_{\text{BCS}} \rangle$  from each term. In Sec. III, we showed that the particle number distribution of a projected wave function  $\rho_N$  is related to the unprojected distribution  $\rho_N^{(0)}$  by

$$\rho_N = g_N \rho_N^{(0)} , \quad (\text{A2})$$

where,

$$g_N \approx C \frac{((L - N/2)!)^2}{L! (L - N)!} .$$

Particle number and number fluctuations of the projected wave function can be derived from Eq. (A2) and Eq. (A1), upon invoking a saddle point approximation. We define a generating function  $\Xi_\lambda$ ,

$$\begin{aligned} \Xi_\lambda &\equiv 2 \prod_k (|u_k|^2 + |v_k|^2 \lambda) \\ &= \sum_{N_\sigma=0}^L \lambda^{N_\sigma} \rho_{2N_\sigma}^{(0)} . \end{aligned} \quad (\text{A3})$$

We invert Eq. (A3) using a contour integral on the complex  $\lambda$ -plane along a circle around  $\lambda = 0$ :

$$\rho_N^{(0)} = \frac{1}{2\pi i} \oint \frac{\Xi_\lambda}{\lambda^{N_\sigma+1}} d\lambda . \quad (\text{A4})$$

Note that, in the integrand, only  $\rho_{2N_\sigma}^{(0)}/\lambda = \rho_N^{(0)}/\lambda$  gives a finite value. The others powers of  $\lambda$  vanishes. Multiplying by  $g_N$  gives

$$\rho_N \approx \frac{1}{2\pi i} \oint g_N \frac{\Xi_\lambda}{\lambda^{N_\sigma+1}} d\lambda . \quad (\text{A5})$$

Eq. (A5) can be written as

$$\rho_N \approx \frac{1}{2\pi i} \oint d\lambda e^{f(\lambda, N)} , \quad (\text{A6})$$

where

$$f(\lambda, N) = \log \Xi_\lambda - \left( \frac{N}{2} + 1 \right) \log \lambda + \log g_N . \quad (\text{A7})$$

Using Stirling's formula,

$$\begin{aligned} \log g_N &\approx 2 \left( L - \frac{N}{2} \right) \log \left( L - \frac{N}{2} \right) - (L - N) \log (L - N) \\ &\quad - L \log L + \log C \end{aligned} \quad (\text{A8})$$

The saddle point  $(\bar{n} = \frac{\bar{N}}{L}, \bar{\lambda})$  of Eq. (A6) is determined

by

$$\begin{aligned} \frac{\partial f}{\partial \lambda} &= \frac{\partial \log \Xi_\lambda}{\partial \lambda} - \frac{\frac{N}{2} + 1}{\lambda} \\ &= \frac{\partial}{\partial \lambda} \sum_k \log (|u_k|^2 + |v_k|^2 \lambda) - \frac{\frac{N}{2} + 1}{\lambda} \\ &= \sum_k \frac{|v_k|^2}{|u_k|^2 + |v_k|^2 \lambda} - \frac{\frac{N}{2} + 1}{\lambda} \\ &\equiv 0 , \end{aligned} \quad (\text{A9})$$

for  $N \gg 1$ ,

$$\begin{aligned} \bar{n} &\approx 2 \frac{\frac{\bar{N}}{2} + 1}{L} \\ &= 2 \frac{1}{L} \sum_k \frac{\bar{\lambda} |v_k|^2}{|u_k|^2 + \bar{\lambda} |v_k|^2} , \end{aligned} \quad (\text{A10})$$

and

$$\begin{aligned} \frac{\partial f}{\partial N} &= -\frac{1}{2} \log \lambda - \log \left( L - \frac{N}{2} \right) + \log (L - N) \\ &\equiv 0 , \end{aligned} \quad (\text{A11})$$

i.e.,

$$\begin{aligned} \bar{\lambda} &= \left( \frac{L - \bar{N}}{L - \frac{\bar{N}}{2}} \right)^2 \\ &= g_t^2 . \end{aligned} \quad (\text{A12})$$

Eq. (A10) and Eq. (A12) lead to Eq. (22),

$$n_{\text{after}} = \bar{n} = \frac{\bar{N}}{L} = 2 \frac{1}{L} \sum_k \frac{g_t^2 |v_k|^2}{|u_k|^2 + g_t^2 |v_k|^2} ,$$

for the average particle density of a projected BCS wave function. Without the factor  $g_N$  this calculation would give the well known result for an unprojected BCS wave function,

$$n_{\text{before}} = \bar{n} = 2 \frac{1}{L} \sum_k |v_k|^2 .$$

To calculate the particle number fluctuations of the projected wave function, we need to expand  $f(\lambda, N)$  up to second order in  $N$  and  $\lambda$  around the saddle point. Then, integration over  $\lambda$  in Eq. (A6) approximates the particle number distribution  $\rho$  by a gaussian distribution, yielding an expression for number fluctuations. With

$$\begin{aligned} f_{\lambda\lambda}(\lambda, N) &\equiv \frac{\partial^2 f}{\partial \lambda^2} \\ &= - \sum_k \frac{|v_k|^4}{(|u_k|^2 + |v_k|^2 \lambda)^2} + \frac{\frac{N}{2} + 1}{\lambda^2} , \\ f_{\lambda N}(\lambda, N) &\equiv \frac{\partial^2 f}{\partial \lambda \partial N} = -\frac{1}{2\lambda} , \\ f_{NN}(\lambda, N) &\equiv \frac{\partial^2 f}{\partial N^2} = \frac{1}{2} \frac{1}{L - \frac{N}{2}} - \frac{1}{L - N} , \end{aligned}$$

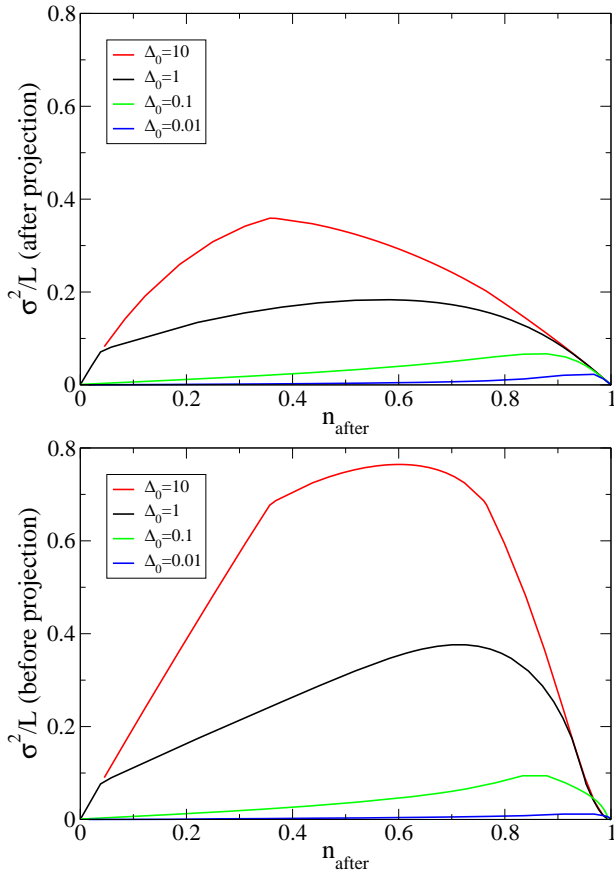


FIG. 5: The fluctuation  $\sigma_{\text{after}}^2/\sigma_{\text{before}}^2$  after/before projection for different values of the order parameter  $\Delta_0 = 0.01/0.1/1/10$ , as a function of the particle density after projection  $n_{\text{after}}$ .

the second order expansion can be written as

$$\begin{aligned} f(\lambda, N) - f(\bar{\lambda}, \bar{N}) \approx & f_{\lambda\lambda}(\bar{\lambda}, \bar{N}) \frac{(\lambda - \bar{\lambda})^2}{2} \\ & + f_{\lambda N}(\bar{\lambda}, \bar{N})(\lambda - \bar{\lambda})(N - \bar{N}) \\ & + f_{NN}(\bar{\lambda}, \bar{N}) \frac{(N - \bar{N})^2}{2}. \end{aligned} \quad (\text{A13})$$

For this level of the saddle point approximation for  $\lambda$ , the contour around  $\bar{\lambda}$  for the integral in Eq. (A6) must be taken so that  $f_{\lambda\lambda}(\bar{\lambda}, \bar{N})(\lambda - \bar{\lambda})^2 < 0$ . Since  $f_{\lambda\lambda}(\bar{\lambda}, \bar{N}) > 0$  and contribution only near the saddle point is relevant, the path is taken from  $\bar{\lambda} - i\infty$  to  $\bar{\lambda} + i\infty$ . By variable transformation  $\lambda = \bar{\lambda} + i\lambda'$ , one can perform a gaussian integral of  $\lambda'$ . Then, we obtain a gaussian distribution for  $\rho_N$ ,

$$\begin{aligned} \rho_N \approx & \frac{1}{2\pi} \int_{-\infty}^{\infty} d\lambda' e^{f(\bar{\lambda} + i\lambda', N)} \\ \approx & \exp \left[ \left( f_{\bar{N}\bar{N}} - \frac{f_{\bar{\lambda}\bar{N}}^2}{f_{\bar{\lambda}\bar{\lambda}}} \right) \frac{(N - \bar{N})^2}{2} \right] e^{f(\bar{\lambda}, \bar{N})}. \end{aligned} \quad (\text{A14})$$

The variance of  $\bar{N}$  (average particle number of a projected BCS wave function) can now be read off from

Eq. (A14). We get,

$$\begin{aligned} \frac{\sigma_{\text{after}}^2}{L} &= -\frac{1}{L} \left( f_{\bar{N}\bar{N}} - \frac{f_{\bar{\lambda}\bar{N}}^2}{f_{\bar{\lambda}\bar{\lambda}}} \right)^{-1} \\ &= 2 \left[ \frac{1}{(1 - \frac{\bar{n}}{2})(1 - \bar{n})} + \frac{1}{\frac{2}{L} \sum_k \frac{\bar{\lambda}|u_k|^2|v_k|^2}{(|u_k|^2 + |v_k|^2\bar{\lambda})^2}} \right]^{-1}, \end{aligned} \quad (\text{A15})$$

where we used Eq. (A10) in the second term. For  $\bar{\lambda}$  we must insert  $g_t^2$ . For completeness, we mention that for the unprojected wave function, *i.e.*  $g_N$  not included, this approach yields the known result

$$\frac{\sigma_{\text{before}}^2}{L} = 4 \frac{1}{L} \sum_k |u_k|^2 |v_k|^2. \quad (\text{A16})$$

The fluctuations  $\frac{\sigma^2}{L}$  are illustrated in Fig. 5 as a function of the particle density after projection  $n_{\text{after}} (= \bar{n})$  for unprojected ( $|\Psi_{\text{BCS}}\rangle$ ) and projected ( $P|\Psi_{\text{BCS}}\rangle$ ) BCS  $d$ -wave functions. As expected, the fluctuations vanish at half filling, since projection freezes the charge degrees of freedom entirely.

## APPENDIX B: GUTZWILLER APPROXIMATION FOR THE $t - J$ HAMILTONIAN

We summarize the Gutzwiller approximation for the so-called 3-site terms in the  $t - J$  model, that are included in the VMC study of Yokoyama and Shiba<sup>14</sup>.

The  $t - J$  model can be derived from a large  $U$  expansion of the Hubbard model. The Hamiltonian is valid in the reduced Hilbert space of no double occupied states, and is given by

$$H_{\text{eff}} = T + H_{\text{eff}}^{(2)} \quad (\text{B1})$$

where

$$T = -t \sum_{\langle i,j \rangle, \sigma} (c_{i,\sigma}^\dagger c_{j,\sigma} + c_{j,\sigma}^\dagger c_{i,\sigma}) \quad (\text{B2})$$

and

$$\begin{aligned} H_{\text{eff}}^{(2)} = & J \sum_{\langle i,j \rangle} \mathbf{S}_i \mathbf{S}_j - \frac{J}{4} \sum_{\langle i,j \rangle} n_i n_j \\ & - \frac{J}{4} \sum_{i, \tau \neq \tau', \sigma} c_{i+\tau, \sigma}^\dagger c_{i, -\sigma}^\dagger c_{i, -\sigma} c_{i+\tau', \sigma} \\ & + \frac{J}{4} \sum_{i, \tau \neq \tau', \sigma} c_{i+\tau, -\sigma}^\dagger c_{i, \sigma}^\dagger c_{i, -\sigma} c_{i+\tau', \sigma}. \end{aligned} \quad (\text{B3})$$

Here,  $J = 4\frac{t^2}{U}$ ,  $\mathbf{S}_i$  are the spin operators on site  $i$ , and  $n_i = n_{i,\uparrow} + n_{i,\downarrow}$  with  $n_{i,\sigma} = c_{i,\sigma}^\dagger c_{i,\sigma}$ .  $\langle i, j \rangle$  are pairs of n.n sites and  $i + \tau$  denotes a n.n. site of  $i$ .

We are interested in the energies  $E^{(1)}$  and  $E^{(2)}$  calculated in Ref. 14:

$$\begin{aligned} E^{(1)} &= \frac{1}{L} \frac{\langle \Psi_{\text{BCS}} | P T P | \Psi_{\text{BCS}} \rangle}{\langle \Psi_{\text{BCS}} | P P | \Psi_{\text{BCS}} \rangle} , \\ E^{(2)} &= \frac{1}{L} \frac{\langle \Psi_{\text{BCS}} | P H_{\text{eff}}^{(2)} P | \Psi_{\text{BCS}} \rangle}{\langle \Psi_{\text{BCS}} | P P | \Psi_{\text{BCS}} \rangle} . \end{aligned} \quad (\text{B4})$$

We invoke the Gutzwiller approximation. The renormalization factors,  $g_t$  for kinetic energy (Eq. (B2)) and  $g_s$  for spin exchange (first term in Eq. (B3)), are given in Eq. (3). The second term of Eq. (B3),  $n_i n_j$ , is not renormalized. The approximation for the 3-site terms (3rd and 4th term of Eq. (B3)) is done as follows ( $|\psi\rangle = P|\psi_0\rangle$ ):

$$\begin{aligned} &\frac{\langle \Psi | c_{i+\tau,\uparrow}^\dagger c_{i,\downarrow}^\dagger c_{i,\downarrow} c_{i+\tau',\uparrow} | \Psi \rangle}{\langle \Psi | \Psi \rangle} \\ &= \frac{\langle \Psi | c_{i+\tau,\uparrow}^\dagger n_{i,\downarrow} (1 - n_{i,\uparrow}) c_{i+\tau',\uparrow} | \Psi \rangle}{\langle \Psi | \Psi \rangle} \\ &= g_3 \frac{\langle \Psi_0 | c_{i+\tau,\uparrow}^\dagger n_{i,\downarrow} (1 - n_{i,\uparrow}) c_{i+\tau',\uparrow} | \Psi_0 \rangle}{\langle \Psi_0 | \Psi_0 \rangle} , \end{aligned} \quad (\text{B5})$$

$$\begin{aligned} &\frac{\langle \Psi | c_{i+\tau,\downarrow}^\dagger c_{i,\uparrow}^\dagger c_{i,\downarrow} c_{i+\tau',\uparrow} | \Psi \rangle}{\langle \Psi | \Psi \rangle} \\ &= g_3 \frac{\langle \Psi_0 | c_{i+\tau,\downarrow}^\dagger c_{i,\uparrow}^\dagger c_{i,\downarrow} c_{i+\tau',\uparrow} | \Psi_0 \rangle}{\langle \Psi_0 | \Psi_0 \rangle} \end{aligned} \quad (\text{B6})$$

The renormalization factor  $g_3$  is derived by considering the number of terms that contribute to the projected and the unprojected side respectively. The projected side (lhs) contributes only if (i) site  $i + \tau$  is unoccupied, *i.e.*, probability  $(1 - n)$ , (ii) site  $i$  is singly occupied by a  $\downarrow$ -electron, *i.e.*, probability  $n_\downarrow$ , and (iii) site  $i + \tau'$  is singly occupied by an  $\uparrow$ -electron, *i.e.*, probability  $n_\uparrow$ . On the other hand, the unprojected side (rhs) in Eq. (B5)/Eq. (B6) contributes only if (i) site  $i + \tau$  is not occupied by an  $\uparrow$ -electron/ $\downarrow$ -electron, *i.e.*, probability  $(1 - n_\uparrow) / (1 - n_\downarrow)$ , (ii) site  $i$  is singly occupied by a  $\downarrow$ -electron, *i.e.*, probability  $n_\downarrow(1 - n_\uparrow)$ , and (iii) site  $i + \tau'$  must have an  $\uparrow$ -electron, *i.e.*, probability  $n_\uparrow$ . These probabilities yield the Gutzwiller factor (ratio of contributions from projected and unprojected states),

$$g_3 = \frac{(1 - n)n_\sigma n_\sigma}{(1 - n_\sigma)n_\sigma(1 - n_\sigma)n_\sigma} = \frac{1 - n}{(1 - n_\sigma)^2} , \quad (\text{B7})$$

where we assumed  $n_\uparrow = n_\downarrow = n_\sigma$ .

We can now write down the renormalized  $t - J$  Hamiltonian  $H'_{\text{eff}}$ ,

$$H'_{\text{eff}} = T' + H'_{\text{eff}}^{(2)} , \quad (\text{B8})$$

where,

$$T' = -g_t t \sum_{\langle i,j \rangle, \sigma} (c_{i,\sigma}^\dagger c_{j,\sigma} + c_{j,\sigma}^\dagger c_{i,\sigma}) , \quad (\text{B9})$$

$$\begin{aligned} H'_{\text{eff}}^{(2)} &= g_s J \sum_{\langle i,j \rangle} \mathbf{S}_i \mathbf{S}_j - \frac{J}{4} \sum_{\langle i,j \rangle} n_i n_j \\ &- g_3 \frac{J}{4} \sum_{i,\tau \neq \tau',\sigma} c_{i+\tau,\sigma}^\dagger n_{i,-\sigma} (1 - n_{i,\sigma}) c_{i+\tau',\sigma} \\ &+ g_3 \frac{J}{4} \sum_{i,\tau \neq \tau',\sigma} c_{i+\tau,-\sigma}^\dagger c_{i,\sigma}^\dagger c_{i,-\sigma} c_{i+\tau',\sigma} . \end{aligned} \quad (\text{B10})$$

By using  $T'$  and  $H'_{\text{eff}}^{(2)}$ , Eq. (B4) ( $E^{(1)}$  and  $E^{(2)}$ ) can be calculated using unprojected wave functions,

$$\begin{aligned} E^{(1)} &= \frac{1}{L} \frac{\langle \Psi_{\text{BCS}} | T' | \Psi_{\text{BCS}} \rangle}{\langle \Psi_{\text{BCS}} | \Psi_{\text{BCS}} \rangle} , \\ E^{(2)} &= \frac{1}{L} \frac{\langle \Psi_{\text{BCS}} | H'_{\text{eff}}^{(2)} | \Psi_{\text{BCS}} \rangle}{\langle \Psi_{\text{BCS}} | \Psi_{\text{BCS}} \rangle} . \end{aligned} \quad (\text{B11})$$

Evaluating Eq. (B11) by Wick's decomposition for a  $d$ -wave BCS state,

$$\frac{E^{(1)}}{t} = -2g_t(\xi_x + \xi_y) ,$$

$$\begin{aligned} \frac{E^{(2)}}{0.25J} &= - (3g_s - 1)(\xi_x^2 + \xi_y^2)/2 \\ &- (3g_s + 1)(|\Delta_x|^2 + |\Delta_y|^2)/2 - 2n^2 \\ &- g_3 n (1 - n_\sigma) (\xi_{2x} + \xi_{2y} + 2\xi_{x-y} + 2\xi_{x+y}) \\ &- g_3 (1 + n_\sigma) (\xi_x^2 + \xi_y^2 + 4\xi_x \xi_y) \\ &- g_3 (2 - n_\sigma) (|\Delta_x|^2 + |\Delta_y|^2 + 4\Re(\Delta_x \Delta_y^*)) , \end{aligned} \quad (\text{B12})$$

where we defined  $(\tau, \tau' = x, y)$

$$\begin{aligned} \xi_\tau &= \sum_\sigma \langle c_{i,\sigma}^\dagger c_{i+\tau,\sigma} \rangle = \frac{1}{L} \sum_k 2 \cos(k_\tau) |v_k|^2 , \\ \xi_{\tau \pm \tau'} &= \sum_\sigma \langle c_{i+\tau,\sigma}^\dagger c_{i \pm \tau',\sigma} \rangle = \frac{1}{L} \sum_k 2 \cos(k_\tau \pm k_{\tau'}) |v_k|^2 , \\ \Delta_\tau &= \langle c_{i,\uparrow}^\dagger c_{i+\tau,\downarrow}^\dagger - c_{i,\downarrow}^\dagger c_{i+\tau,\uparrow}^\dagger \rangle = \frac{1}{L} \sum_k 2 \cos(k_\tau) v_k u_k^* . \end{aligned}$$

The last three rows in Eq. (B12) correspond to the 3-site terms of the  $t - J$  model and are renormalized by the Gutzwiller factor  $g_3$ .

<sup>1</sup> P. W. Anderson (private communication) and P. W. Anderson and N. P. Ong, cond-mat/0405518.

<sup>2</sup> R. B. Laughlin, cond-mat/0209269.

<sup>3</sup> M. C. Gutzwiller, Phys. Rev. Lett. **10**, 159 (1963).

<sup>4</sup> Claudio Gros, Phys. Rev. B **38**, 931 (1988).

<sup>5</sup> F. C. Zhang, C. Gros, T. M. Rice and H. Shiba, Supercond. Sci. Tech. **1** 36 (1988); also available as cond-mat/0311604.

<sup>6</sup> P. W. Anderson, P. A. Lee, M. Randeria, T. M. Rice, N. Trivedi and F. C. Zhang, J. Phys. Cond. Mat. **16** R755 (2004).

<sup>7</sup> A. Paramekanti, M. Randeria and N. Trivedi, Phys. Rev. Lett. **87** 217002 (2001); Phys. Rev. B **69** 144509 (2004); Phys. Rev. B **70**, 054504 (2004).

<sup>8</sup> C. Gros, R. Joynt, T.M. Rice, Phys. Rev. B **36**, 381 (1987).

<sup>9</sup> Jörg Bünemann, Florian Gebhard, Torsten Ohm, Stefan Weiser, and Werner Weber, cond-mat/0503332; D. Jaksch, C. Bruder, J. I. Cirac, C. W. Gardiner, and P. Zoller, Phys. Rev. Lett. **81** 3108 (1998); M. Bak and R. Micnas, J. Phys.: Cond. Matt. **10**, 9029 (1998); B. R. Bulka and S. Robaszkiewicz, Phys. Rev. B **54**, 13138 (1996). Jian Ping Liu, Phys. Rev. B **49**, 5687 (1994); Daniel S. Rokhsar and B. G. Kotliar, Phys. Rev. B **44**, 10328 (1991); K. Seiler, C. Gros, T. M. Rice, K. Ueda, D. Vollhardt, J. Low. Temp. Phys. **64**, 195 (1986).

<sup>10</sup> N. Fukushima, B. Edegger, V.N. Muthukumar, C. Gros, cond-mat/0503143.

<sup>11</sup> J.Y. Gan, Y. Chen, Z B. Su, F.C. Zhang, Phys. Rev. Lett. **94**, 067005 (2005).

<sup>12</sup> D. Vollhardt, Rev. Mod. Phys. **56**, 99 (1984).

<sup>13</sup> Several extensions to the Gutzwiller approximation have been proposed in the literature. See, for instance, M. Ogata and A. Himeda, J.Phys. Soc. Jpn. **72**, 374 (2003); G. Seibold, and J. Lorenzana, Phys. Rev. Lett. **86**, 2605 (2001); M. Lavagna, Phys. Rev. B **41**, 142 (1990).

<sup>14</sup> H. Yokoyama, and H. Shiba, J. Phys. Soc. Jpn. **57**, 2482 (1988).

<sup>15</sup> By infinite system size, we mean that the sum over all  $\mathbf{k}$  in Eq. (22) is transformed into an integral. In the VMC studies the sum over  $\mathbf{k}$  is considered on a finite system, *i.e.*, a finite number of  $\mathbf{k}$ -values. Generally the resulting finite size effects are small<sup>16</sup>, and a direct comparison to an infinite system is reasonable.

<sup>16</sup> H. Yokoyama, and M. Ogata, J. Phys. Soc. Jpn. **65**, 3615 (1996).